Aggregation of an α-Helical Transmembrane Peptide in Lipid Phases, Studied by Time-Resolved Fluorescence Spectroscopy

ARTICLE *in* THE JOURNAL OF PHYSICAL CHEMISTRY B · SEPTEMBER 1999

Impact Factor: 3.3 · DOI: 10.1021/jp9904116

4 AUTHORS, INCLUDING:

Göran Lindblom
Umeå University
232 PUBLICATIONS **7,720** CITATIONS

Aggregation of an α-Helical Transmembrane Peptide in Lipid Phases, Studied by Time-Resolved Fluorescence Spectroscopy

Stein-Tore Bogen,[‡] Gerda de Korte-Kool,[†] Göran Lindblom,[‡] and Lennart B.-Å. Johansson*[,‡]

Biophysical Chemistry, Department of Chemistry, Umeå University, S-901 87 Umeå, Sweden, and Department of Biochemistry of Membranes and Enzymology, Institute of Biomembranes, Utrecht University, 3584 CH Utrecht, The Netherlands

Received: February 4, 1999; In Final Form: July 14, 1999

The aggregation of octadecyl rhodamine 101 (R*h*101C_{18}) and a Rh101-labeled transmembrane peptide (Rh101WALP16) solubilized in lipid phases was studied. Different lipid phases in excess of water were formed with either 1,2-dimyristoyl-*sn*-glycero-3-phosphocholine (DMPC), 1,2-dioleoyl-*sn*-glycero-3-phosphocholine (DOPC), or 1,2-dierucoyl-*sn*-glycero-3-phosphochline (DErPC). Rh101 was covalently attached with its carboxyl group to the C-terminal ethanolamine. Time-resolved polarized fluorescence spectroscopy was used to determine the fluorescence relaxation and anisotropy at molar ratios ranging from 1 Rh101-derivative per 5000 lipids (1:5000) to 1 Rh101-derivative per 50 lipids (1:50). At concentrations of the Rh101-derivatives exceeding about 1 mol %, the fluorescence intensity is quenched, and the fluorescence lifetime is significantly decreased. This is compatible with electronic energy transfer to ground-state dimers of Rh101groups. The time-resolved fluorescence decays were analyzed by analytical models of donor−acceptor electronic energy transfer. The models account for energy transfer between Rh101 monomers (donors) and Rh101dimers (acceptors), spatially distributed in one and two dimensions. For the amphiphilic Rh101C_{18} molecules solubilized in DMPC, DOPC, and DErPC, the fluorescence relaxation is very well described as energy transfer in lipid vesicles between donors and acceptors, distributed on the inner and outer surfaces of the bilayer. For statistical reasons, pairs of molecules in contact are more likely to appear at high concentrations. Hereafter these are referred to as statistical dimers. It is found that the dimer concentration of Rh101C_{18} in the bilayer of the various lipids, is slightly above that calculated for statistical dimers. In contrast, the dimerization of Rh101WALP16 is five- to 10-fold increased, as compared to the expected concentration of statistical dimers. This suggests that the transmembrane peptide has an inherent affinity for aggregation in lipid bilayers formed by DMPC, DOPC, and DErPC. The fluorescence relaxation of Rh101WALP16 in DMPC and DOPC is very well described as donor−acceptor energy transfer across the lipid bilayer of vesicles. However, the fluorescence relaxation of Rh101WALP16 in DErPC is not compatible with energy transfer in lipid bilayers. Instead, a better description is achieved by assuming that the Rh101WALP16 molecules are aggregated along parallel lines. Such a spatial distribution is compatible with recent studies showing a reversed hexagonal phase (H_{II}) that appears at high WALP16 concentrations in DErPC (J. A. Killian et al., *Biochemistry* **1996**, *35*, 1037).

Introduction

Several fundamental processes in biological cells involve the interplay between lipids and membrane proteins. A typical example is the partitioning of proteins into membranes and their subsequent folding.[1−8] To get an understanding of protein/lipid and peptide/lipid interactions and how lipids possibly affect the activity of integral membrane proteins, we have begun to investigate the behavior of very hydrophobic peptides mimicking transmembrane segments of integral membrane proteins.[9−11] One of the synthetic peptides that we have chosen to work with has the following amino acid sequence HCO−AWW$(LA)_5$-WWA−$NHCH_2CH_2OH$, (WALP16). This artificial peptide is designed to be a model for transmembrane segments of integral membrane proteins. It consists of 16 amino acid residues, contains no charges, and is anchored to the polar/nonpolar interface of phospholipid bilayers by two tryptophans at each end of the peptide. WALP16 has a strong ability to induce nonbilayer structures in phosphatidylcholine/water mixtures, provided that the hydrophobic thickness of the lipid aggregates is sufficiently large.[9,11]

Besides obtaining information about the liquid crystalline structure of the peptide/lipid/water system and the three-dimensional structure of the peptide itself, we are interested in the peptide−peptide and peptide−lipid interactions that occur within a membrane. This is still largely unknown, despite several extensive investigations of transmembrane hydrophobic peptides solubilized in lipid bilayers.[9,12−24] A first step of our studies was therefore to determine the phase diagram of hydrophobic peptides and membrane lipids over a large interval of concentrations, and it was found that a number of different nonlamellar phases are formed in such systems.[11] These phase diagrams suggest that peptide/peptide aggregation may occur in the lamellar phase, before the transition to a nonlamellar phase. The present work aims at providing details about the possible aggregation of WALP16 in lipid phases.

* Corresponding author. Telephone: 46-(0)90-786 5149. Telefax: 46-(0)90-786 7779. E-mail: Lennart.Johansson@chem.umu.se.
‡ Umea University.
† Utrecht University.

10.1021/jp9904116 CCC: $18.00
Published on Web 09/10/1999

To reveal and quantify the aggregation of peptide molecules in lipid phases is not a straightforward task by any spectroscopic method (see ref 25 for a recent review). However, fluorescence spectroscopy is one of the most promising sensitive methods for such investigations, because some chromophoric molecules undergo dimerization in their electronic ground state. Usually these dimers are nonfluorescent and quench the fluorescence of excited monomers. If the quenching mechanism is electronic energy transfer, it is possible to derive models that relate the process at a molecular level to experiments.[26,27] A similar approach might be used in ESR spectroscopy by making use of short-range spin−spin interactions between spin labels.[28−31]

In the present study we apply electronic energy transfer to investigate aggregation among the WALP16 peptides that were labeled with rhodamine 101 (Rh101) at the C-terminal position. This is the first time that models describing donor-to-acceptor energy transfer are used to characterize peptide−peptide interaction in lipid phases. The models were adopted to analyze the fluorescence relaxation, as monitored by time-correlated single-photon counting (TCSPC) spectroscopy. Xanthene dyes, like Rh101, are known to form ground-state dimers[32,33] at high *local* concentrations.[32] This situation occurs if macromolecules labeled with the dye form aggregates, and it provides a basic idea of this study. Within an aggregate two adjacent Rh101 groups can form a dimer that acts as an excitation trap (acceptor) of monomeric Rh101 groups (donors). According to Förster's theory of electronic energy transfer,[34] the rate of transfer depends strongly on distance ($1/R^6$), as well as *spatial* distribution of the interacting donor and acceptor molecules. To account for the spatial dimension, models based on the Förster mechanism were previously developed and tested.[27,35,36] In this work these models were applied to determine the local concentration of Rh101−WALP16 dimers in lipid bilayers formed by 1,2-dimyristoyl-*sn*-glycero-3-phosphocholine (DMPC), 1,2-dioleoyl-*sn*-glycero-3-phosphocholine (DOPC), and 1,2-dierucoyl-*sn*-glycero-3-phosphochline (DErPC).

Experimental Section

Materials. 1,2-dimyristoyl-*sn*-glycero-3-phosphocholine (DMPC), 1,2-dioleoyl-*sn*-glycero-3-phosphocholine (DOPC), and 1,2-dierucoyl-*sn*-glycero-3-phosphochline (DErPC) were purchased from Avanti Polar Lipids and used without further purification. Rhodamine 101 octadecyl ester ($Rh101C_{18}$) was purchased from Molecular Probes, Inc.

N,*N*-dicyclohexylcarbodiimide (DCC) and 4-pyrolidinopyridin (PPY) were purchased from Aldrich Chemie. DCC and PPY were dried from benzene and stored under vacuum before use. Rhodamine 101 was purchased from Lambda Physik.

Synthesis and Purification of WALP16. WALP16 was synthesized as described previously[9] and was a kind gift of Drs. R. E. Koeppe II and D. V. Greathouse. The peptide was purified on an HPLC column packed with Nucleosil Si 100−10 (Machery Nagel) using chloroform/methanol/water (75/15/1, v/v/v) as eluent.

Preparation of Rh101−WALP16. Rh101−WALP16 was prepared by covalently coupling the carboxyl group of Rh101 to the hydroxyl group of the C-terminal ethanolamine of WALP16. Purified WALP16 [10 mg (≈ 5 μmol)] was dissolved in 1.3 mL of a mixture of benzene and pyridin (2:1, by volume). Both solvents were freshly dried over an Al_2O_3 column. Next, a 5-fold molar excess was added of PPY and 10-fold molar excesses of DCC and Rhodamine 101. The resulting mixture was homogenized by vortexing and subsequently stored in the dark under N_2 at room temperature. The reaction was followed by HPTLC on silica using chloroform:methanol:water (80:20:1, by volume) as eluent, in which the R_f value of WALP16 is 0.4. The spots were visualized by heating the HPTLC plates after spraying with 10% H_2SO_4 in water. After one night of incubation all WALP16 had disappeared, as judged from the HPTLC plates, and a new product was formed with an R_f of 0.6. Benzene (1 mL) was added and the mixture was applied to a silica column (silica gel 40 μm, Baker) with chloroform:methanol:water (80:20:1, by volume) as eluent. Small fractions were collected and analyzed with HPTLC. The product-containing fractions were combined, dried, and redissolved in 1 mL of eluent. The product was further purified on an HPLC packed with Lichhrosorb Si60 (Chrompack) using chloroform:methanol:water (150:25:1 by volume) as eluent. Analysis by mass spectrometry showed that the product has the expected mass of 2370 D. The degree of labeling of WALP16 was calculated by using absorption spectroscopy and the known molar absorptivity of different Rh101 derivatives.[37] Known amounts of the lyophilized Rh101-labeled peptide were dissolved in ethanol, and the absorption spectra were measured. The degree of labeling was found to be 43.3 ± 1.2%.

Preparation of Small Unilamellar Vesicles (SUV). Small unilamellar vesicles of DOPC, DMPC, and DErPC, containing Rh101-derivatives at different molar ratios were prepared by sonication. Vesicles containing solubilized $Rh101C_{18}$ ester were prepared as follows. Dry lipid was dissolved in an organic solvent and mixed with appropriate amounts of $Rh101C_{18}$ dissolved in ethanol. For dissolving DOPC and DErPC, ethanol was used, while dichloromethane was better suited for DMPC. The solvent was removed under a stream of N_2(g), and the remaining film dried at 320 K and 0.1 Torr for 12 h. This was followed by addition of 3 mL of HEPES buffer at pH 7, and the suspension was repeatedly (10 times) frozen in liquid N_2 and thawed. At this stage the sample was stored in a freezer prior to sonication. Suspension of lipids and Rh101−WALP16 was prepared by another method, as described elsewhere.[9,38] The freeze−thawed samples were sonicated in short intervals (10 s of sonication and 20 s for rest) during 90 min. During sonication the samples were kept at constant temperature well above the gel to liquid-phase transition. The sonicator, a Soniprep 150 (MSE Scientific Instruments, UK) was equipped with an exponential microprobe. The amplitude used was 8−10 μm. After sonication, the samples were centrifuged at 4500 x *g* for 15 min and the supernatant was used for experiments. In all experiments the samples were either thermostated at 293 K (DOPC and DErPC) or at 303 K (DMPC).

Fluorescence and Absorption Spectra. The fluorescence spectra were recorded using a SPEX Fluorolog 112 (SPEX Ind., New Jersey) equipped with Glan−Thompson polarizers. The spectral bandwidths were 5.5 and 2.7 nm for the excitation and emission monochromators, respectively. To calibrate the spectrometer, a standard lamp from the Swedish National Testing and Research Institute (Borås, Sweden) was used. All fluorescence spectra were corrected. The fluorescence intensity was monitored with the excitation and emission polarizers set relative to a laboratory fixed Cartesian frame (*X*,*Y*,*Z*). The excitation polarizer was set parallel with the *Z*-axis, while the emission polarizer was set at the magic angle (54.7°) relative to the *Z*-axis. The fluorescence steady-state anisotropy was monitiored with other polarizer settings, the details are outlined elsewhere.[39] Absorption spectra were recorded on a GBC 920 spectrophotometer (GBC, Inc., Australia).

Time-Correlated Single-Photon Counting (TCSPC). The fluorescence lifetime and time-resolved fluorescence depolar-

ization decays were obtained using a Rhodamine 6G dye laser (Spectra Physics model 375) synchronously pumped by a mode-locked Nd: YAG laser (Spectra-Physics model 3400). To reduce the repetition rate to about 800 kHz, an extra-cavity pulse-picker was used. The excitation polarizer setting parallel (*Z*), perpendicular (*Y*), or at the magic angle (*M*) with respect to the laboratory *Z*-axis, was adjusted by means of a Glan−Thompson polarizer and a Soleil−Babinet compensator. The emission was monitored after passing a Glan−Thompson polarizer adjusted parallel to the *Z*-axis. The samples were excited at 585 nm, and the emission was observed through a long pass filter (at $\lambda > 610$ nm). A microchannel plate (MCP, model R1564U-01, Hamamatsu, Japan) was used for detecting the emitted photons. The instrument was operated in the reversed mode. The stop signal, that is the excitation pulse, was detected by using a fast photodiode (PD). To avoid pile-up distortion, the excitation beam was attenuated so that the detected emission events was at a rate less than 1.5% of the repetition excitation frequency.[40] The outputs of the MCP and PD were routed through constant fraction discriminators (Ortec, model 9307) into the time-to-amplitude-converter (TAC, Ortec model 567). By an analogue-to-digital converter, the TAC output was transferred into a number that was stored in a multichannel analyzer (Nuclear Data, USA). The number of data channels were 4096, and their width was 19.2 ps/channel. The fwhm of the instrument response function was about 130 ps.

Data Analysis. The data analysis was carried out on an Intel based PC, running the Red Hat Linux 5.0 operating system (Red Hat Inc.). All models were implemented with a FORTRAN program, and compiled with the GNU Fortran compiler (g77 v0.5.18). The quality of the fit between a model and the data was judged on the basis of the statistical test parameters χ^2 and Durbin−Watson (DW), as well as by plotting the residuals.

Fluorescence Quenching Experiments. At high concentrations (typically > mM) xanthene dyes tend to form dimers, which show absorption spectra [32,41,42] of different strength and band shape as compared to the monomer. Usually the dimers are very weakly fluorescent. When solubilized in lipid vesicles, the *local* concentration can be sufficiently high for dimerization, although the *total* concentration is several order of magnitude lower. In the presence of dimers, the fluorescence intensity decreases, but recovers upon dissolving the aggregates. By adding detergents to rhodamines solubilized in lipid vesicles, the aggregates of rhodamines as well as lipids dissolve. Hereby, monomers of rhodamine are distributed among a large number of micelles.[43] In present studies, the corrected fluorescence spectra were measured before and after addition of sodium dodecyl sulfate (SDS) in water (100 μL 30 w/w % SDS). The resulting increase of the fluorescence intensity is used to estimate the fraction of Rh101 dimers. This is possible because for each dissolved dimer, two fluorescent Rh101 moieties form.

Förster Radius of Energy Transfer from Rh101 Monomers to R101 dimers in Vesicles. To calculate the Förster radius, the absorption spectrum of Rh101 dimers is required. However, it is not a straightforward task to determine $\epsilon_{\text{dimer}}(\nu)$. To the best of our knowledge, the dimer spectrum of Rh101 has not been reported. An approximate value of the Förster radius was calculated by using the dimer spectrum of RhB.[42] It is then assumed that the molar absorptivity [$\epsilon(\nu)$] of the dimers of RhB and the Rh101 are very similar, which should be a good approximation.[44] To calculate the Förster radius, the dimeric absorption spectrum was shifted (on a scale of wavenumbers). The shift with respect to the absorption spectrum of Rh101 derivatives solubilized in the lipid phases was adjusted to be the same as for RhB. Notice, the spectral shapes of Rh101 and RhB are almost identical. From the overlap between the shifted dimer spectrum and the corrected fluorescence spectrum of Rh101, the Förster radius (R_0) was calculated.[39] For dimers of Rh101 solubilized in lipid phases, we obtained $R_0 = 47 \pm 2$ Å.

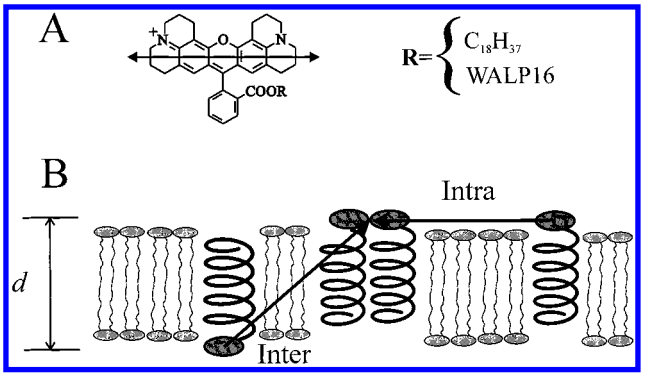

Figure 1. (A) The structure formula of Rh101. The arrow indicates the direction of the electronic transition dipole moment corresponding to the $S_0 \leftrightarrow S_1$ electronic transitions. (B) Schematic of possible intra and inter monolayer paths of electronic energy migration between an excited Rh101WALP16 monomer and a Rh101WALP16 dimer.

TCSPC Decays. The observed fluorescence decay curve, $F_{\text{exp}}(t)$, is a convolution of the true decay function, $F(t)$, and the instrumental response function, $E(t)$:

$$F_{\text{exp}}(t) = A\int_0^t E(t-\tau)F(\tau)\mathrm{d}\tau$$

where the constant A depends on the number of photons collected. The decay curves were analyzed using a nonlinear least-squares analysis, that implements an iterative re-convolution and a modified Levenberg−Marquardt algorithm.[45,46]

Models of Energy Transfer

In a lipid bilayer the polar Rh group of rhodamine derivatives, such as $Rh101C_{18}$, is localized in the lipid-water interface (See Figure 1), while the hydrophobic part (C_{18}) resides in the hydrocarbon region.[26,39,47] The electronic transition dipole moment, polarized in the plane of the rhodamine molecule (See Figure 1), tends to be perfectly oriented parallel to the lipid bilayer surface.[48] The orientation of the Rh101 groups of WALP16 monomers and dimers as well as the dimers of $Rh101C_{18}$ in lipid bilayers is assumed to be parallel to the lipid bilayer. Previous studies show that a slightly different order has a minor influence on the parameters determined.[26] Furthermore, the theory of energy transfer suggests a weak dependence of the average molecular order.[27] Within an ensemble of $Rh101C_{18}$ molecules solubilized in lipid bilayers, energy transfer can occur across the bilayer, as well as within each monolayer. The electronic energy transfers from excited Rh101 molecules to dimers of Rh101. Hence, the dimers are acceptors, or in a more general terminology, they are quenchers of the fluorescence emission.

For energy transfer in one dimension (i.e., on a line, $\Delta = 1$) and in two dimensions (i.e., within a monolayer, $\Delta = 2$) among molecules whose transition dipoles are randomly oriented in a plane, the probability ($G^{\text{s}}_{\Delta,\text{intra}}(t)$) of an initially excited monomer to be excited at a time t later is given by[27]

$$\ln G^{\text{s}}_{\text{l,intra}}(t) = -C_1\left(\frac{15}{8}\right)^{1/6}\Gamma\left(\frac{5}{6}\right)\left(\frac{t}{\tau}\right)^{1/6} \qquad (1a)$$

$$\ln G^{s}_{2,\mathrm{intra}}(t) = -C_2\left(\frac{15}{8}\right)^{1/3}\Gamma\left(\frac{2}{3}\right)\left(\frac{t}{\tau}\right)^{1/3} \quad (1b)$$

These equations are strictly valid in the dynamic limit and for electronic transition dipoles oriented in a plane, and spatially distributed in one ($\Delta = 1$, eq 1a) or two ($\Delta = 2$, eq 1b) dimensions. The reduced surface concentration of acceptors, the fluorescence lifetime in the *absence* of acceptors, and the gamma function are denoted by C_Δ, τ, and $\Gamma(x)$, respectively. The reduced concentration in one dimension is the average number of acceptor molecules along a line defined by twice the Förster radius. The reduced concentration in two dimensions means the average number of acceptor molecules within the area of a circle defined by the Förster radius. Hence, for a number density of quenchers (ρ), the reduced concentrations in one and two dimensions are given by $C_1 = \rho 2R_0$ and $C_2 = \pi\rho R^2$.

For energy transfer between two parallel monolayers with in-plane randomly oriented transition dipoles, spatially distributed in one and two dimensions, the excitation probability is given by[27]

$$\ln G^{s}_{1,\mathrm{inter}}(\mu) = -\frac{C_1}{6\nu}\int_0^1 \left\{1 - \exp\left[-\mu\left(\frac{5}{4}s - 3s^{4/3} + \frac{9}{4}s^{5/3}\right)\right]\right\} s^{-7/6}\,\mathrm{d}s \quad (2a)$$

$$\ln G^{s}_{2,\mathrm{inter}}(\mu) = -\frac{C_2}{3\nu^2}\int_0^1 \left\{1 - \exp\left[-\mu\left(\frac{5}{4}s - 3s^{4/3} + \frac{9}{4}s^{5/3}\right)\right]\right\} s^{-4/3}\,\mathrm{d}s \quad (2b)$$

In eqs 2a and b, $\mu = (3/2)t\nu^6\tau^{-1}$, $s = \cos^6\theta_r$, and $\nu = R_0 d^{-1}$, where d stands for the distance between the monolayers, which is approximately equal to the thickness of a lipid bilayer (see Figure 1). The angle θ_r, is between the surface normal and a line connecting the center of mass of each interacting dipole. Particular attention must be paid to the numerical evaluation of the integrals in eq 2. To handle the singularity at $s = 0$, two consecutive partial integrations were performed. This ensures terms on the form of s^α ($\alpha \geq 0$) appear only in the integrand. Because the numerical evaluation of this integral is time-consuming it is divided into 5 subintervals, for which analytical functions were fitted. The excitation probability for each interval is described by a sum of exponential functions.

The total excitation probability $\{G^s(t)\}$ is the joint probability of intra $\{G^s_{\Delta,\mathrm{intra}}(t)\}$and inter $\{G^s_{\Delta,\mathrm{inter}}(t)\}$ processes, that is;

$$G^s(t) = G^s_{\Delta,\mathrm{intra}}(t)G^s_{\Delta,\mathrm{inter}}(t) \quad (3)$$

In the absence of excitation traps, the fluorescence relaxation of the donor molecules is accurately fitted to

$$F(t) = \sum_{j=1}^{2} \alpha_j \exp(-t/\tau_j) \quad (4)$$

In the presence of dimers both eqs 3 and 4 must be used to describe the total fluorescence relaxation according to:

$$F(t) = G^s(t)\sum_{j=1}^{2} \alpha_j \exp(-t/\tau_j) \quad (5)$$

To model energy transfer between Rh101 and its dimers in lipid bilayers, analyses were separately performed for excitation probabilities of the intralayer transfer (eq 1) and interlayer transfer (eq 2), as well as their combination (eq 3).

Results and Discussion

Fluorescence Quenching. Lipid samples of DMPC, DOPC, and DErPC were prepared in an excess of water at molar dye: lipid ratios ranging from 1:50 to 1:5000. With increasing $Rh101C_{18}$ or Rh101WALP16 concentration, dimers are more likely formed. However, the dimer concentration should exceed the statistically expected concentration of contact pairs (hereafter called statistical pairs). This is because Rh dyes spontaneously dimerize in water and alcohols, typically at millimolar concentrations.[32,33,42]

Upon adding detergents to lipid phases in excess of water, micelles are formed. Thereby, the Rh101 derivatives are spread over a large number of micelles. As a consequence, the probability of dimer formation is largely reduced.[43] The ratio of the fluorescence intensity recorded before and after adding the detergent is a qualitative measure on the degree of quenching, and the amount of quenching dimers. Typical quenching data obtained for $Rh101C_{18}$ and Rh101WALP16 at various molar ratios in DMPC are summarized in Figure 2A. The highest quenching is observed at 2 mol % of Rh101WALP16, but it depends on the phospholipid, and decreases in the order DMPC > DErPC > DOPC.

The quenching experiments strongly suggest that the fraction of Rh101WALP16 dimers in the different lipid phases is significantly enhanced, as compared to that of $Rh101C_{18}$. Although the Rh101 moiety possesses an inherent tendency for dimerization, the larger fraction of Rh101WALP16 dimers is hardly explained by Rh101−Rh101 interactions. More likely the aggregation is related to the hydrophobic part (WALP16) of the peptide.

Photophysics of Rh101. The fluorescence relaxation of Rh101 in solvents is monoexponential. For instance, $Rh101C_{18}$ in *n*-decanol and ethanol shows fluorescence lifetimes of $\tau =$ 4.3 and 4.6 ns, respectively.[37] In lipid phases, the photophysics is more complex, even at low $Rh101C_{18}$ concentrations, but it is very well described by a sum of two exponential functions, with a dominating lifetime of 4.7 ns (≈95%), and a shorter component of about 0.5 ns. The fluorescence decay of Rh101WALP16 in vesicles is also double exponential with a dominating lifetime of 4.7 ns (≈80%) and second component of about 1.7 ns. A detailed explanation to the more complex relaxation in vesicles is not available. However, chromophores residing in a lipid−water interface are subject to strong local gradient of polarity. Depending on their specific location and orientation in this gradient, the fluorescence lifetime may differ, and hence there is a distribution of lifetimes. As a result, the observed fluorescence decay is likely not a monoexponential function. The resulting ensemble average over such a micro-heterogeneous distribution is here *effectively* described by a sum of two exponential functions. For both Rh101 derivatives, the average lifetime was calculated from the fluorescence relaxation decay monitored for the most diluted samples (1:5000). This mean value was used in the analyses below (cf. eqs 1 and 2). A more complete analysis would involve the distribution of lifetimes. Such an extended analysis accounting for lifetime distributions would include more parameters, which are difficult to determine unambiguously.

Fluorescence Anisotropy and Lifetimes. The fluorescence anisotropy monitors rotational motions and local order of the fluorescent group. In addition, it depends on the rate of energy transfer from an excited molecule to molecules of the same, or

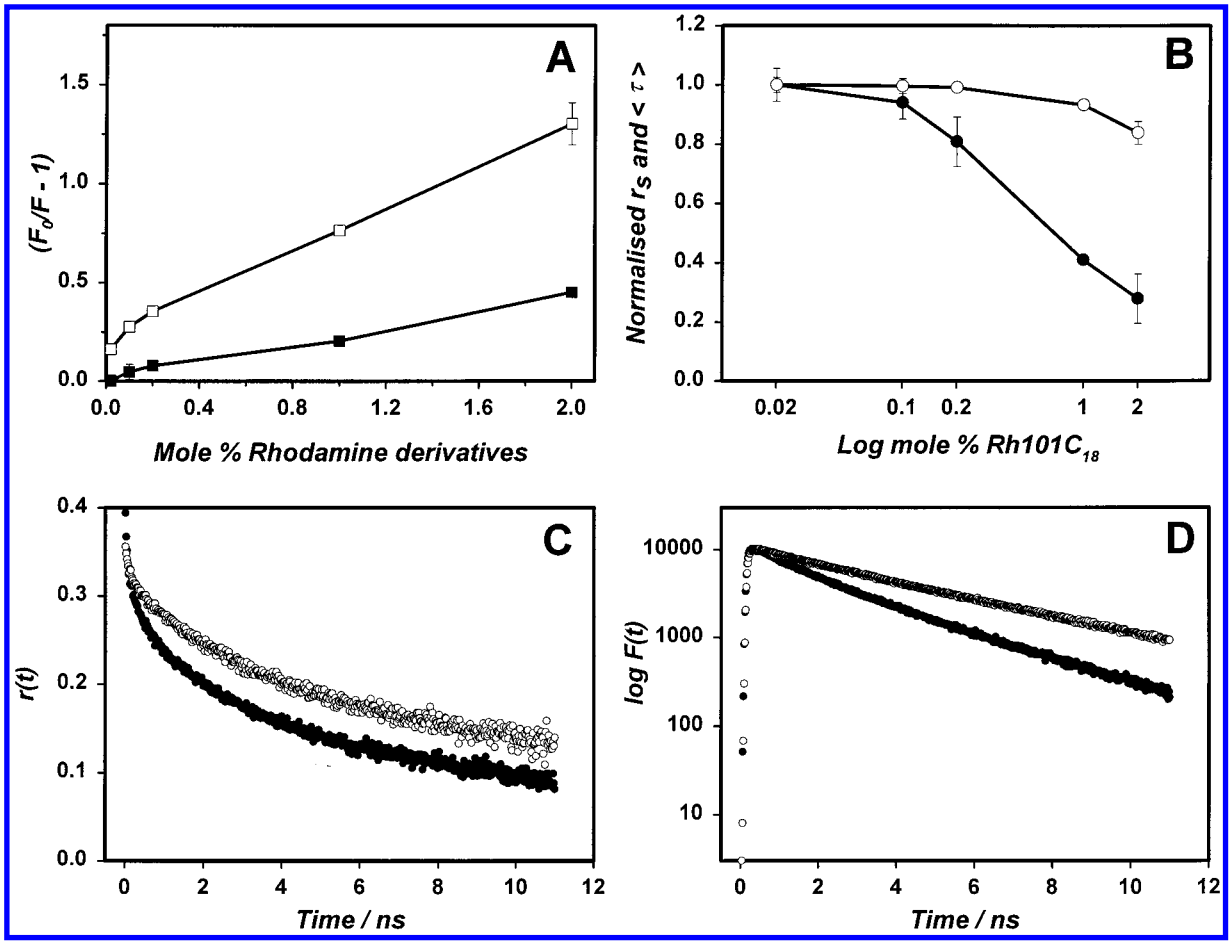

Figure 2. (A) The fluorescence quenching (F_0/F) of $Rh101C_{18}$ (■), and Rh101WALP16 (□) solubilized in DMPC vesicles. (B) The normalized average fluorescence lifetime ($\langle\tau\rangle$, ○) and steady-state fluorescence steady-state anisotropy (r_s, ●) as a function of the concentration (mole %) of $Rh101C_{18}$ in DMPC vesicles. (C) Time-resolved fluorescence anisotropy ($r(t)$) of $Rh101C_{18}$ solubilized in DMPC vesicles at the dye-to-lipid ratio of 1:5000 (○), and 1:500 (●). (D) The time-resolved fluorescence relaxation ($F(t)$) of Rh101WALP16 in DMPC vesicles at the dye-to-lipid ratio of 1:5000 (○), and 1:50 (●). Note in (C), the fluorescence anisotropy is constructed by combining the measured decays for different polarizations. In (D), the decays represent the convolution of the true fluorescence decay and the instrumental response function (not shown).

of a different kind. Electronic energy transfer among molecules of the same kind is usually called donor−donor energy migration. However, energy migration among donors does not influence the fluorescence lifetime, while the decay rate of the fluorescence anisotropy is increased. The fluorescence anisotropy, obtained at moderate and low concentrations of $Rh101C_{18}$ and Rh101WALP16 in vesicles, is compatible with donor−donor energy migration. As is exemplified in Figure 2B, the fluorescence steady-state anisotropy decreases upon increasing concentration of $Rh101C_{18}$ in DMPC vesicles, which is expected for donor−donor energy migration. The average fluorescence lifetime is almost constant at mole fractions below 1 mol %, as is shown in Table 1. Notice, at mole fractions above 1 mol %, the fluorescence lifetime is significantly decreased. The latter is compatible with electronic energy transfer to excitation traps, i.e., dimers of Rh101.

Further support of energy migration and transfer is obtained from a combined consideration of the time-resolved fluorescence anisotropy and lifetime data (See Figure 2C,D). There is a more rapid initial decay of the fluorescence anisotropy at the $Rh101C_{18}$ to DMPC ratio of 1:500, as compared that of 1:5000, while the average fluorescence lifetime remains about the same. This implies that energy migration is more efficient at the higher concentration, as is also expected because the average distance is shorter between interacting molecules. The almost identical decay rates observed at times longer than about 2 ns, show that the local mobility of the Rh101 group is not significantly influenced by concentration.

The effect on the fluorescence relaxation with increasing

TABLE 1: Mean Fluorescence Lifetimes ($\langle\tau\rangle$ [a]) Obtained for $Rh101C_{18}$ and Rh101WALP16 in Lipids of DMPC, DOPC, and DErPC[b]

lipid	$\langle\tau\rangle$/ns of Rh101WALP16	$\langle\tau\rangle$/ns of $Rh101C_{18}$
	DMPC	
1/50.	2.81 ± 0.12	3.99 ± 0.02
1/100	3.29 ± 0.06	4.43 ± 0.01
1/500	4.07 ± 0.05	4.71 ± 0.01
1/1000	4.27 ± 0.04	4.73 ± 0.01
1/5000	4.45 ± 0.02	4.75 ± 0.01
	DOPC	
1/50	3.43 ± 0.13	4.00 ± 0.05
1/100	3.81 ± 0.02	4.42 ± 0.01
1/500	4.40 ± 0.01	4.71 ± 0.01
1/1000	4.51 ± 0.01	4.75 ± 0.01
1/5000	4.56 ± 0.01	4.78 ± 0.01
	DErPC	
1/50.	3.72 ± 0.05	4.09 ± 0.02
1/100	3.80 ± 0.01	4.45 ± 0.01
1/500	4.23 ± 0.05	4.63 ± 0.01
1/1000	4.33 ± 0.01	4.70 ± 0.04
1/5000	4.47 ± 0.02	4.70 ± 0.02

[a] $\langle\tau\rangle = \sum_{j=1}^{2} \alpha_j\tau^2_j / \sum_{j=1}^{2} \alpha_j\tau_j$. [b] For different mixtures, the molar ratio of $Rh101C_{18}$ and labelled Rh101WALP16 to lipid is given. The errors are given as the standard error of the mean.

TABLE 2: Distances (*d*) between Layers of Interacting Monomers and Dimers of Rh101 As Obtained by Using the Models Presented in the Section "Models of Energy Transfer"[a]

system	*d*/Å	$d_{bilayer}$/Å	model
$Rh101C_{18}$/DMPC	39.7 ± 0.4	34.5[c]	2D inter & intra
$Rh101C_{18}$/DOPC	40.1 ± 0.2	38[b]	2D inter & intra
$Rh101C_{18}$/DErPC	40.2 ± 0.2	45.6[d]	2D inter & intra
Rh101WALP16/DMPC	32.8 ± 0.7	34.5[c]	2D inter
Rh101WALP16/DOPC	41.6 ± 0.8	38	2D inter
Rh101WALP16/DErPC	54.7 ± 3.8	45.6[d]	2D inter & intra
Rh101WALP16/DErPC	41 ± 2	45.6[d]	1D inter & intra

[a] 1D and 2D refer to energy transfer in one and two dimensions. Inter and intra means the model used to analyze the data is accounting for inter and intra monolayer contributions. The errors are given as the standard error of the mean. [b] From X-ray diffraction experiments.[53] [c] From X-ray diffraction experiments.[54] [d] Estimated by extrapolating the distances obtained by X-ray diffraction for DPPC[54] and DOPC.

Rh101WALP16 concentration is illustrated in Figure 2D. For the most concentrated system (1:50), the $F(t)$ decay is no doubt faster and nonexponential. As a result of electronic energy transfer to excitation traps, the *average* lifetime also decreases from 4.5 ns to about 2.8 ns (See Table 1).

Inter and Intra Monolayer Energy Transfer in $Rh101C_{18}$−Lipid Bilayers. The fluorescence relaxation decays were analyzed by models accounting for pure intralayer, pure interlayer, as well as, the combined inter and intra layer energy transfer. The best description of data was achieved for a combination of inter and intra monolayer energy transfer (eqs 3 and 4). Two variables, C_2 and ν enter the analyses as fitting parameters. The reduced concentration depends on the Förster radius of donor−acceptor transfer and the number density of acceptor molecules. The traps are assumed to be dimers of Rh101 with a calculated Förster radius of $R_0 = 47$ Å. For further details in determining R_0, see the Experimental Section. The number density of dimers can be calculated if the concentration of *randomly* distributed dimers is known. The second parameter, ν, depends on the shortest possible distance (d) between a Rh101 monomer and a Rh101−Rh101 dimer that are localized on opposite sides of a lipid bilayer. Since rhodamine dyes prefer to reside in the lipid−water interface,[26,39,47] the distance d provides an estimate of the lipid bilayer thickness. To extract statistically reliable values on the parameters C_2 and ν, a prerequisite is a significant shortening of the average fluorescence lifetime (See Table 1). In this context, "reliable" means that the parameters extracted are not sensitive to the choice of initial values chosen in the convolution analyses. This is not feasible at molar ratios of $Rh101C_{18}$:lipid exceeding about 1:100. The values reported in Tables 2 and 3 refer to average values obtained from two to five independent experiments with the dye:lipid ratios of 1:100 and 1:50. The d values agree reasonably well with independently determined values of the lipid bilayer thicknesses (see Table 2). For several reasons, a perfect agreement is not expected. For example, the planar Rh101 moiety may take different angles of tilt with respect to the normal of the lipid bilayer, although the orientation of the electronic transition dipole maintains an almost perfect orientation parallel to the plane of the bilayer. Notice, there is no way to obtain a statistically acceptable analysis by forcing the distance to be fixed at say 20 or 50 Å, while the reduced concentration is used as a fitting parameter. However, it is possible to obtain an acceptable fit to the data by using a fixed value of d equal to the bilayer thickness. In the latter approach, the C_2 values show only minor deviations from those obtained with d as a floating parameter.

At 2 mol % (1:50) of $Rh101C_{18}$ in vesicles of DMPC, DOPC, and DErPC, the reduced concentrations are varying between 0.2 and 0.25. These values correspond to approximately 1 $Rh101C_{18}$-dimer per 30000 Å^2, or to about 17 dimers in a vesicle with an average area of 500 000 Å^2. From simulation studies[49] it is possible to estimate the average number of statistical dimers,[50] and in its extension, the reduced concentration of dimer excitation traps, C_2. These studies yield that $C_2 \approx 0.21$ at 2 mol % of statistically distributed $Rh101C_{18}$ molecules. For $Rh101C_{18}$ the experimental C_2 values obtained with DMPC and DOPC are slightly higher than statistically expected. This is compatible with an inherent tendency of dimerization, in agreement with the well-known fact that xanthene derivatives form dimers, at mM concentrations. Moreover, at 1−2 mol % in lipid bilayers, the estimated *local* Rh101-concentration is also in the order of mM.

In previous work, donor−donor energy migration among lissamine RhB−phosphatidyl ethanol amine lipids in DOPC vesicles was investigated.[26] The influence of dimerization was negligible at dye-to-DOPC ratios of less than 1:500. To account for the combined inter and intra monolayer energy migration in the analyses of the time-resolved fluorescence anisotropy, models analogous to eqs 1−2 were used. The d-values thus obtained agree very well with the bilayer thickness, as well as a random spatial distribution of the RhB molecules. The latter was concluded because the C_2 values obtained from the analyses were in perfect agreement with the independently calculated values for a random distribution of the RhB−lipids.

Inter and Intra Monolayer Energy Transfer in Rh101-WALP16−Lipid Bilayers. To analyze the fluorescence relaxation of Rh101WALP16 in vesicles composed of either DMPC, DOPC, or DErPC, the models accounting for pure intralayer, pure interlayer transfer, as well as their combination were used. However, none of the models describe satisfactory Rh101WALP16 in DErPC at the ratio of 1:50 and 1:100. At the moment, we therefore leave their analyses for the next subsection.

For the lipid phases of DMPC and DOPC the model of *inter* monolayer transfer provides the best fit to data (See Figure 3). It means, the statistical test parameters judging on the deviation between model and data are good, but also that the values of d are in reasonable agreement with the thickness of the lipid bilayers known from independent experiments (see Tables 2 and 3). Attempts to use an alternative model that includes a partition coefficient of intra and inter monolayer energy transfer, does not provide much improvement on the statistical test parameters. By using this model it is found that the reduced dimer concentration (C_2) of intra monolayer transfer cannot exceed about 10% of the reduced concentration of inter monolayer transfer. Consequently, to a major extent energy transfer is from monomeric Rh101WALP16 molecules, located with their rhodamine moiety on one monolayer, to Rh101WALP16 dimers located with their rhodamine moiety at the opposite monolayer. The significantly smaller area of the inner monolayer of a vesicle, as compared to the outer one, is a possible reason for this asymmetry. The inner radius of small unilamellar vesicles of DOPC is about 100 Å,[51] and for the same number Rh101WALP16 peptides oriented toward the inside and the outside of a vesicle, the number density in the interior monolayer is then about twice as high, relative to the outside monolayer. For such an asymmetric number density it is expected that the electronic energy is to a major extent transferred from the outer to the inner monolayer of the DMPC and DOPC vesicles. The reduced dimer concentrations obtained (See Table 3) are typically five to 10-fold higher, as compared to those of

TABLE 3: The Reduced Concentrations (C_Δ, $\Delta = 1$ or 2) Obtained by Using the Models Presented in the Section "Models of Energy Transfer"[a]

system	C_Δ 2.0 mol % Rh101	C_Δ 1.0 mol % Rh101	model
$Rh101C_{18}$/DMPC ($\Delta = 2$)	0.24 ± 0.01	0.10 ± 0.01	2D inter & intra
$Rh101C_{18}$/DOPC ($\Delta = 2$)	0.25 ± 0.02	0.11 ± 0.01	2D inter & intra
$Rh101C_{18}$/DErPC ($\Delta = 2$)	0.20 ± 0.01	0.07 ± 0.01	2D inter & intra
statistical dimers in DMPC (2D)	0.218	0.072	
statistical dimers in DOPC (2D)	0.209	0.069	
Rh101WALP16/DMPC ($\Delta = 2$)	1.30 ± 0.02	0.97 ± 0.02	2D inter
Rh101WALP16/DOPC ($\Delta = 2$)	1.30 ± 0.16	0.92 ± 0.03	2D inter
Rh101WALP/DErPC ($\Delta = 2$)	0.30 ± 0.01	0.24 ± 0.01	2D inter & intra
Rh101WALP/DErPC ($\Delta = 1$)	0.55 ± 0.03	0.46 ± 0.01	1D inter & intra

[a] 1D and 2D refer to energy transfer in one and two dimensions. Inter and intra means the model used to analyze the data is accounting for inter and intra monolayer contributions. The reduced concentration of statistical dimers was obtained from simulation studies.[50] The errors are given as the standard error of the mean.

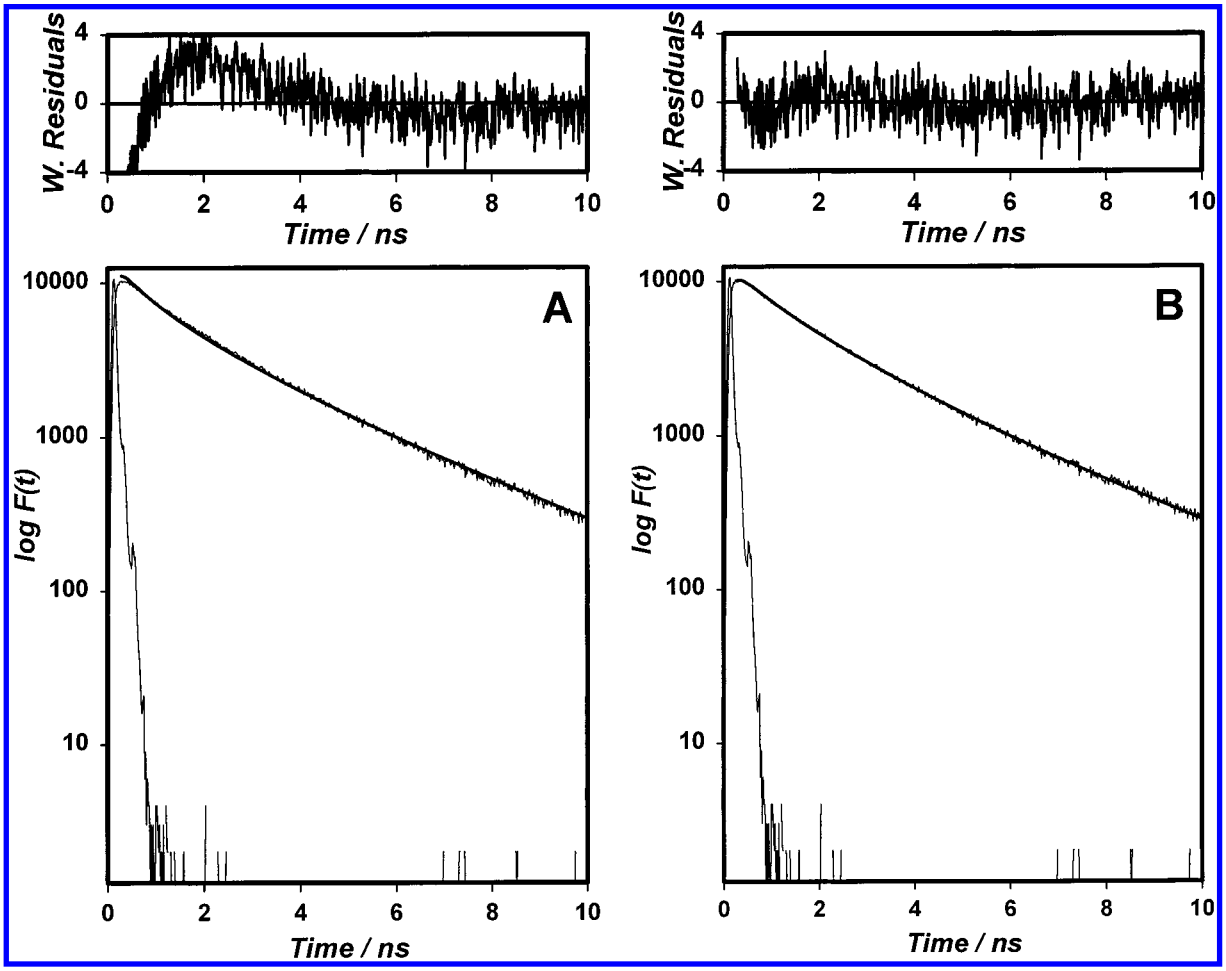

Figure 3. Fitting between a model that accounts for intra and inter monolayer energy transfer (A), as well as inter bilayer transfer (B) and the fluorescence decay ($F(t)$). Data were obtained for Rh101WALP16 solubilized in DMPC vesicles, at a dye-to-lipid ratio of 1:50. The instrumental response function is shown for each of the decays. The weighted residuals are given above each $F(t)$ decay. The statistical test parameters, χ^2 and DW (Durbin−Watson) are 2.11 and 1.21 for fit (A), and 1.21 and 1.98 for fit (B), respectively.

$Rh101C_{18}$. This implies the number of Rh101WALP16 dimers per unit area is significantly higher than of $Rh101C_{18}$ as well as the predicted statistical dimers. The fluorescence quenching results further support this conclusion. Taken together, the fluorescence relaxation strongly suggests a substantial aggregation of Rh101WALP16 in bilayers of DMPC and DOPC, energetically favored by the hydrophobic WALP16 moieties.

Rh101WALP16 Mixed with DErPC. To understand the difficulties in analyzing the data of Rh101WALP16 in DErPC at the ratios of 1:50 and 1:100, it is necessary to consider previous phase equilibrium studies of different lipids mixed with WALP16.[9] In DMPC and DOPC a lamellar phase is formed at WALP16 concentrations of less than one WALP16 per 25 lipids (1:25). However at this ratio for DErPC, the presence of a reversed hexagonal phase (H_{II}) cannot be excluded. Because the degree of Rh101-labeled WALP16 is only about 50% (cf. the Experimental Section), the actual *total* amount of peptide in the most concentrated sample is about 1:25. This implies that the model assuming energy transfer in two-dimensional bilayers of DErPC is not adequate. Thus, it is neither surprising to find *d*-values incompatible with the thickness of the lamellar phase of DErPC (Table 2), nor to find that the statistical test

parameters are nonacceptable. For WALP16 peptides distributed in the H_{II} phase, as was previously suggested by Killian et al.,[9] it is reasonable to use a model that combines energy transfer among Rh101 molecules spatially distributed along two parallel lines. This corresponds to one-dimensional, or intra line energy transfer, as well as inter line energy transfer from donors to acceptors localized on two parallel lines separated at a distance (*d*). The distance is about the thickness of a lipid bilayer of DErPC. Indeed, the model adapted to the H_{II} phase provides much more reasonable *d*-values (see Tables 2 and 3). Although the statistical parameters used for judging on the quality of fitting between the model and the data are not perfect, they are significantly better, as compared to those obtained with the model of inter and intramonolayer energy transfer in 2D. The reason for the less than perfect statistical parameters is likely a *mixture* of two phases, dominated by H_{II} in equilibrium with a lamellar phase. Furthermore, this is supported by the better description of the one-dimensional model at the ratio of 1:50, as compared to 1:100.

Rh101WALP16, as a Model of WALP16. When using fluorescent probes to monitor properties of a system where the fluorophores are not naturally present, it is always important to consider the possibility that the probe itself may induce artifacts. Here we are interested in whether the hydrophobic WALP16 peptide has an intrinsic affinity of self-aggregation in lipid bilayers. Because Rh101 forms dimers, it is important to ensure that the Rh101WALP16 aggregates are *not* caused by the Rh101−Rh101 aggregation. To investigate this, the aggregation of $Rh101C_{18}$ was separately studied and compared with the appearance of statistical dimers. It is clear that the concentration of $Rh101C_{18}$ dimers is slightly higher than expected for statistical reasons, while the concentrations of Rh101WALP16 dimers are five- to 10-fold increased. This suggests that the hydrophobic moiety (i.e., the WALP16 part) has an intrinsic affinity for self-aggregation. A recent study of WALP16 in different diacylphosphocholine bilayers, doped with a spin-labeled fatty acid, does not exclude the formation of dimers or small oligomers.[52] Further support for the assumption that Rh101WALP16 mimics the behavior of WALP16, is the difficulty in satisfactorily describing energy transfer at high Rh101WALP16 concentrations if one assumes that DErPC forms a lamellar phase (as in lipid vesicles). A much better description is obtained by using a model that accounts for the H_{II} phase. Moreover, the *d* values found are quite reasonable.

Conclusions

At high molar ratios of the amphiphilic dye, $Rh101C_{18}$, in lipid vesicles of DMPC, DOPC, and DErPC, ground-state dimers are formed. By their presence, the fluorescence relaxation of $Rh101C_{18}$ is quenched. The fluorescence relaxation is quantitatively described by a model that accounts for intra and inter monolayer energy transfer. The analyses of data provide distances between the interacting monolayers in reasonable agreement with the thickness of the different lipid bilayers. As could be expected, the dimer concentration obtained from the analyses are somewhat higher than the values theoretically predicted.

Energy transfer to the dimeric forms of Rh101WALP16 in DMPC and DOPC vesicles is best described by a model which predominantly accounts for inter monolayer transport. This finding is compatible with an asymmetric number density of excitation traps between the outer and inner monolayers.

Energy transfer from monomers to dimers of Rh101WALP16 in DErPC at high concentrations (i.e., a dye-to-lipid molar ratio of 1:50 and 1:100) is best described by assuming a spatially *one*-dimensional distribution of the Rh101WALP16 molecules in an H_{II} phase.

The results obtained for the DMPC and DOPC systems at the highest concentrations strongly suggest that an aggregation of *at least* one dimer per 3000−6000 $Å^2$. This is most probably an underestimate, because the actual total WALP16 peptide concentration is about twice that of Rh101WALP16. As a whole, the time-resolved fluorescence experiments suggest that the hydrophobic WALP16 peptide has an inherent tendency of self-aggregation.

Acknowledgment. We are grateful to Mrs. Eva Vikström for skillful technical assistance, to Drs. Maria Sperotto and J. Antoinette Killian for valuable discussions, and to Drs. Roger E. Koeppe II and Denise V. Greathouse for their gift of WALP16. This work was supported by the Kempe Foundations and the Swedish Natural Science Research Council.

References and Notes

(1) Chung, L. A.; Thompson, T. E. *Biochemistry* **1996**, *35*, 11343.
(2) Baumgärtner, A. *Biophys. J.* **1996**, *71*, 1248.
(3) Engelman, D. M.; Seitz, T. A.; Goldman, A. *Annu. Rev. Biophys. Biophys. Chem.* **1986**, *15*, 321.
(4) Popot, J. P.; Vitry, C.; Atteia, A. *Membrane Protein Structure*; White, S. H., Ed.; Oxford University Press: New York, 1994; p 41.
(5) Hunt, J. F.; Rath, P.; Rothschild, K. J.; Engelman, D. M. *Biochemistry* **1997**, *36*, 15177.
(6) Hunt, J. F.; Earnest, T. N.; Bousche, O.; Kalghatgi, K.; Reilly, K.; Horvath, C.; Rothschild, K. J.; Engelman, D. M. *Biochemistry* **1997**, *36*, 15156.
(7) White, S. H. *Membrane Protein Structure*; White, S. H., Ed.; Oxford University Press: New York, 1994; p 97.
(8) Heijne, G. v. *FEBS Lett.* **1994**, *346*, 69.
(9) Killian, J. A.; Salemink, I.; Planque, M. R. R. d.; Lindblom, G.; Koeppe, R. E.; Greathouse, D. V. *Biochemistry* **1996**, *35*, 1037.
(10) Morein, S.; Trouard, T. P.; Hauksson, J. B.; Rilfors, L.; Arvidson, G.; Lindblom, G. *Eur. J. Biochem.* **1996**, *241*, 489.
(11) Morein, S.; Strandberg, E.; Killian, J. A.; Persson, S.; Arvidson, G.; Koeppe, R. E.; Lindblom, G. *Biophys. J.* **1997**, *73*, 3078.
(12) Davis, J. H.; Hodges, R. S.; Bloom, M. *Biophys. J.* **1982**, *37*, 170.
(13) Epand, R. M.; Shai, Y.; Segrest, J. P.; Anantharamaiah, G. M. *Biopolymers* (*Peptide Science*) **1995**, *37*, 319.
(14) Greathouse, D. V.; Hinton, J. F.; Kim, K. S.; Koeppe, R. E. *Biochemistry* **1994**, *33*, 4291.
(15) Huschilt, J. C.; Hodges, R. S.; Davis, J. H. *Biochemistry* **1985**, *24*, 1377.
(16) Killian, J. A.; Prasad, K. U.; Urry, D. W.; Kruijff, B. d. *Biochim. Biophys. Acta* **1989**, *978*, 341.
(17) Pauls, K. P.; MacKay, A. L.; Södermann, O.; Bloom, M.; Tanjea, A. K.; Hodges, R. S. *Eur. Biophys. J.* **1985**, *12*, 1.
(18) Roux, M. R.; Neumann, J. M.; Hodges, R. S.; Devaux, P. F.; Bloom, M. *Biochemistry* **1989**, *28*, 2313.
(19) Echteld, C. J. A. v.; Kruijff, B. d.; Verkleij, A. J.; Leunissen-Bijvelt, J.; Gier, J. d. *Biochim. Biophys. Acta* **1982**, *692*, 126.
(20) Watnick, P. I.; Chan, S. I.; Dea, P. *Biochemistry* **1990**, *29*, 6215.
(21) Xing, J.; Scott, H. L. *Biochim. Biophys. Acta* **1992**, *1106*, 227.
(22) Zhang, Y.-P.; Lewis, R. N. A. H.; Hodges, R. S.; McElhaney, R. N. *Biochemistry* **1992**, *31*, 11579.
(23) Zhang, Y.-P.; Lewis, R. N. A. H.; Henry, G. D.; Sykes, B.; Hodges, R. S.; McElhaney, R. N. *Biochemistry* **1995a**, *34*, 2348.
(24) Zhang, Y.-P.; Lewis, R. N. A. H.; Hodges, R. S.; McElhaney, R. N. *Biochemistry* **1995b**, *34*, 2362.
(25) Lindblom, G.; Quist, P.-O. *Curr. Opin. Colloid Interface Sci.* **1998**, *3*, 499.
(26) Medhage, B.; Mukthar, E.; Kalman, B.; Johansson, L. B.-Å.; Molotkovsky, J. G. *J. Chem. Soc., Faraday. Trans.* **1992**, *88* (19), 2845.
(27) Baumann, J.; Fayer, M. D. *J. Chem. Phys.* **1986**, *85*, 4087.
(28) Voss, J.; Salwinski, L.; Kaback, H. R.; Hubell, W. L. *Proc. Natl. Acad. Sci. U.S.A.* **1995**, *92*, 12295.
(29) Voss, J.; Hubbell, W. L.; Kaback, H. R. *Proc. Natl. Acad. Sci. U.S.A.* **1995**, *92*, 12300.
(30) Rabenstein, M. D.; Shin, Y.-K. *Proc. Natl. Acad. Sci. U.S.A.* **1995**, *92*, 8329.
(31) Farahbakhsh, Z. T.; Huang, Q.-L.; Ding, L.-L.; Altenbach, C.; Steinhoff, H.-J.; Horwitz, J.; Hubbell, W. L. *Biochemistry* **1995**, *34*, 509.
(32) Drexhage, K. H. *Dye Lasers*, Vol. 1; Schäfer, F. P., Ed.; Springer-Verlag: Berlin, 1990; p 155.

(33) Penzkofer, A.; Lu, Y. *Chem. Phys.* **1986**, *103*, 399.
(34) Förster, T. *Ann. Phys.* (*Leipzig*) **1948**, *2*, 55.
(35) Kalman, B.; Johansson, L. B. A. *J. Phys. Chem.* **1992**, *96*, 185.
(36) Johansson, L. B. A.; Engstroem, S.; Lindberg, M. *J. Chem. Phys.* **1992**, *96*, 3844.
(37) Karolin, J.; Bogen, S. T.; Johansson, L. B.-Å.; Molotkovsky, J. G. *J. Fluoresc.* **1995**, *5*, 279.
(38) Killian, J. A.; Trouard, T. P.; Greathouse, D. V.; Chupin, V.; Lindblom, G. *FEBS Lett.* **1994**, *348*, 161.
(39) Bogen, S.-T.; Karolin, J.; Molotkovsky, J. G.; Johansson, L. B.-Å. *J. Chem. Soc., Faraday Trans.* **1998**, *94*, 2435.
(40) Birch, D. J. S.; Imhof, R. E. *Topics in Fluorescence Spectroscopy*, Vol. 1; Lakowicz, J. R., Ed.; Plenum Press: New York, 1991; p 1.
(41) Arbeloa, F. L.; Ojeda, P. R.; Arbeloa, I. L. *J. Photochem. Photobiol., A* **1988**, *45*, 313.
(42) Gál, M. E.; Kelly, G. R.; Kurucsev, T. *J. Chem. Soc., Faraday Trans. 2* **1973**, *69*, 395.
(43) Hoekstra, D.; Boer, T. d.; Klappe, K.; Wilschut, J. *Biochemistry* **1984**, *23*, 5675.
(44) Drexhage, K. H., personal communication, 1998.
(45) Levenberg, K. *Quart. Appl. Math.* **1944**, *2*, 164.
(46) Marquardt, D. W. *J. Soc. Ind. Appl. Math.* **1963**, *11*, 431.
(47) Johansson, L. B. A.; Niemi, A. *J. Phys. Chem.* **1987**, *91*, 3020.
(48) Karolin, J.; Bogen, S.-T.; Johansson, L. B.-Å.; Molotkovsky, J. G. *J. Fluoresc.* **1995**, *5*, 279.
(49) Sperotto, M. M. *Eur. Biophys. J.* **1997**, *26*, 405.
(50) Sperotto, M. M, personal communications, 1998.
(51) Johansson, L. B.-Å.; Kalman, B.; Wikander, G.; Fransson, Å.; Fontell, K.; Bergensthål, B.; Lindblom, G. *Biochim. Biophys. Acta* **1993**, *1149*, 285.
(52) Planque, M. R. R. d.; Greathouse, D. V.; Koeppe, R. E.; Schäfer, H.; Marsh, D. *Biochemistry* **1998**, *37*, 9333.
(53) Bergenståhl, B. A.; Stenius, P. *J. Phys. Chem.* **1987**, *91*, 5944.
(54) Lis, L. J.; McAlister, M.; Fuller, N.; Rand, R. P.; Parsegian, V. A. *Biophys. J.* **1982**, *37*, 657.